Gamma-ray study of pion-induced reactions on the nickel isotopes

H. E. Jackson, S. B. Kaufman, D. G. Kovar, L. Meyer-Schützmeister, K. E. Rehm,* J. P. Schiffer,† S. L. Tabor,‡
S. E. Vigdor,§ and T. P. Wangler

Argonne National Laboratory, Argonne, Illinois 60439

L. L. Rutledge, Jr.‖ and R. E. Segel**

Northwestern University, Evanston, Illinois 60201

R. L. Burman, P. A. M. Gram, R. P. Redwine, and M. A. Yates-Williams

Los Alamos Scientific Laboratory, Los Alamos, New Mexico 87545

The spectra of residual nuclides following 100-, 160-, and 220-MeV π^+ and π^- bombardment of ^{58,60,62,64}Ni have been measured by detecting prompt and, at 220 MeV, β-delayed gamma rays. A wide spectrum of residual nuclides extending along the valley of stability down to Ca, is seen. Where radioactivities were measured, the total (prompt + delayed) observed cross section amounted to ≈ 900 mb. The mean number of nucleons removed increased from about 5 for the ^{58}Ni target to about 8 for ^{64}Ni. The residual nuclide spectrum depends sensitively on the target neutron excess, but is essentially independent of pion charge or pion energy in the range observed. A Monte-Carlo cascade-evaporation calculation involving an intermediate Δ resonance reproduces the yield of residual nuclides far (more than about eight nucleons) removed from the target, but it fails to reproduce the yield of nearer nuclides which is a more sensitive measure of the early stages of the reaction.

NUCLEAR REACTION ^{58,60,62,64}Ni$(\pi^\pm, x\gamma)$, $E_\pi = 100$, 160, 220 MeV; measured prompt and β-delayed γ spectra; determined yields of residual nuclides and their distribution; established systematics. Enriched targets.

I. INTRODUCTION

The new generation of intermediate-energy accelerators provides pion beams of high purity and intensity. With these beams, detailed studies of pion-induced nuclear reactions become feasible. The reactions are complex, beginning with an initial interaction in which a large amount of energy may be transferred to one or more nucleons. A pion can transfer only a relatively small fraction of its kinetic energy in a single collision with a nucleon, but if it is absorbed, its 140-MeV rest mass, in addition to all of its kinetic energy, will be imparted to the nucleus. This initial interaction is followed by a preequilibrium phase in which more nucleons may share the energy and several high-energy nucleons, and possibly other fragments, are emitted. The remaining highly-excited nucleus then decays by particle evaporation into bound states which finally decay by γ emission.

The present work is a study of the systematics of the distribution of the residual nuclides undertaken in the expectation that it would help constrain the basic mechanisms of pion-nucleus interactions. Even-even nuclides were usually identified from

their prompt γ rays, odd-odd and some odd-A nuclides by their radioactivities.

Several experiments have now been reported[1-6] in which intermediate-energy nuclear reactions have been studied by measuring the spectrum of prompt γ rays accompanying such reactions. For nuclei with $A \sim 60$ it appears feasible with this technique to identify $\sim 60\%$ of the estimated total reaction cross section. When induced activities are also measured, it becomes possible to identify $\gtrsim 80\%$ of the total reaction cross section. In a previous communication a study of pion and proton reactions with ^{58}Ni and ^{60}Ni targets was reported.[5] The present work is concerned mainly with pion-induced reactions, and data are presented on the heavier nickel isotopes, ^{62}Ni and ^{64}Ni, as well as some new results on ^{58}Ni.

The present work, combined with that previously published, forms a considerable body of data from which various trends can be extracted. Specifically, the dependence of the distribution of final nuclei on pion energy, pion charge, and target atomic number have been examined and are discussed below. A companion study[7] of pion-induced proton and deuteron spectra from some of the same tar-

gets is also available. In addition, Sadler et al.[8] have studied the distribution of residual nuclides from proton-induced reactions on the Ni isotopes.

II. EXPERIMENTAL RESULTS

Pions from the low-energy-pion (LEP) channel at the Clinton P. Anderson Meson Physics Facility bombarded targets of about 5 g/cm^{2} which were viewed at 90° by a 50-cm[3] Ge(Li) detector whose face was ~13 cm from the center of the beam. The detector was surrounded by a graded shield with ~15 cm of borated polyethylene. In addition to the procedure followed in the earlier measurements to obtain absolute cross sections,[9] in the present run the incident pion flux was measured by activating a piece of plastic at the target position and measuring the induced 20-min ^{11}C activity. The number of incident pions determined using the measured[10] cross sections for forming ^{11}C from ^{12}C agreed to within 5% with that determined by the other method wherein the anode current was integrated from a photomultiplier tube which viewed a scintillator in the pion beam.[11]

A typical run lasted about four hours with an integrated pion flux of about 3×10^9. The γ-ray resolution was about 3 keV and frequent energy calibrations showed gain shifts to be negligibly small over periods of several days. The energy of a strong, well-isolated line could be determined with an accuracy of about ±1 keV. The detector's efficiency was determined with the aid of calibrated sources, and corrections were made for γ absorption in the target. The errors in the absolute cross sections for specific transitions are of the order of 20%.

Spectra were accumulated during both the 500 μs beam bursts and the 8 ms beam-off intervals; the latter showed no lines of significant strength. For each beam energy and charge, a background spectrum was measured with no target. Figure 1 shows the γ-ray spectrum for 160-MeV π^+ on ^{62}Ni. The background lines are identified from the no-target
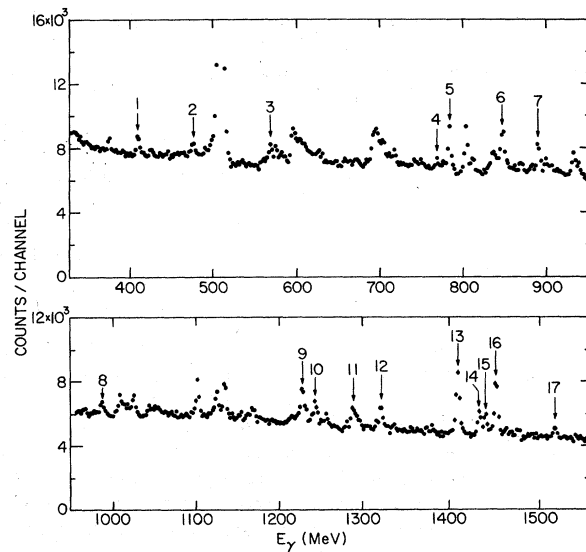

FIG. 1. The spectrum of γ rays from 220-MeV π^+ on ^{58}Ni. The number of counts in each channel has been multiplied by the γ-ray energy to approximately compensate for the detector efficiency. The numbered lines are identified in Table I, other strong lines are a part of the background.

spectrum and are believed to be mainly from interactions of fast neutrons in the detector and surrounding material. Table I lists and identifies the lines observed in all of the Ni spectra. The distribution of final nuclides deduced from the observed spectra are shown in Table II.

It has been previously noted[5] that inelastic transitions in the target nucleus are excited to a significant degree by neutrons originating within the target. The approximate number of such neutrons can be deduced from the yield of residual nuclides and the spectra of energetic nucleons,[7] and it is estimated that 50 to 100% of the observed yield of inelastic transitions may be attributed to secon-

TABLE I. The γ rays observed following pion bombardment of Ni. The numbers in the column labeled "ID" identify the γ-ray lines in Fig. 1. The remaining γ rays in this table without "ID" numbers were observed with targets of other Ni isotopes as indicated in the "Target A" column.

ID	E_γ (keV)	Target A	Nuclide	$J^\pi \rightarrow J_F^\pi$
	340	60,62	^{59}Ni	$\frac{5^-}{2} \rightarrow \frac{3^-}{2}$
1	411	58,60,62	^{55}Fe	$\frac{1^-}{2} \rightarrow \frac{3^-}{2}$
	465	60,62	^{59}Ni	$\frac{1^-}{2} \rightarrow \frac{3^-}{2}$

TABLE I. *(Continued).*

ID	E_γ (keV)	Target A	Nuclide	$J^\pi \to J_F^\pi$
2	478	58,60	^{55}Fe	$\frac{7-}{2} \to \frac{5-}{2}$
	556	64	^{60}Co	$(3^+) \to 5^+$
3	576	58,60,62	^{56}Co	$(4^+) \to 4^+$
	749	58	^{51}Cr	$\frac{3-}{2} \to \frac{7-}{2}$
4	769	58	^{57}Ni	$(\frac{5-}{2}) \to \frac{3-}{2}$
5	783	58,60,62	^{50}Cr	$2^+ \to 0^+$
	811	62,64	^{58}Fe	$2^+ \to 0^+$
	824	64	^{60}Fe	$2^+ \to 0^+$
	826	60,62,64	^{60}Ni	$2^+ \to 0^+$
6	847	58,60,62,64	^{56}Fe	$2^+ \to 0^+$
7	889	58,60,62	^{46}Ti	$2^+ \to 0^+$
	929[a]	62,64	^{51}V	$\frac{3-}{2} \to \frac{7-}{2}$
	931[a]	58,60,62,64	^{55}Fe	$\frac{5-}{2} \to \frac{3-}{2}$
8	983	58,60,62,64	^{48}Ti	$2^+ \to 0^+$
	1099	60,62,64	^{59}Co	$\frac{3-}{2} \to \frac{7-}{2}$
	1157[a]	62	^{44}Ca	$2^+ \to 0^+$
	1163[b]	58	^{51}Cr	$\frac{5-}{2} \to \frac{7-}{2}$
	1164	62,64	^{62}Ni	$4^+ \to 2^+$
	1167[b]	58,60	^{55}Mn	$\frac{11-}{2} \to \frac{7-}{2}$
	1172[c]	62,64	^{62}Ni	$2^+ \to 0^+$
	1186[a]	62,64	^{61}Ni	$\frac{3-}{2} \to \frac{3-}{2}$
	1190[a]	60,62,64	^{59}Co	$(\frac{9-}{2}) \to \frac{7-}{2}$
	1204	62,64	^{61}Co	$\frac{5-}{2} \to \frac{7-}{2}$
9	1224	58,60,62,64	^{57}Co	$\frac{9-}{2} \to \frac{7-}{2}$
10	1238	58,60,62,64	^{56}Fe	$4^+ \to 2^+$
11	1283	58,60,62	^{47}Ti	$\frac{11-}{2} \to \frac{7-}{2}$
12	1316	58,60,62,64	^{55}Fe	$(\frac{5-}{2}) \to \frac{3-}{2}$
	1333	60,62,64	^{60}Ni	$2^+ \to 0^+$
	1348	64	^{64}Ni	$2^+ \to 0^+$
	1378	58,60	^{57}Co	$\frac{3-}{2} \to \frac{7-}{2}$
	1397	58,60	^{47}Ti	$\frac{11-}{2} \to \frac{7-}{2}$
13	1408[d]	58,60,62	^{54}Fe	$2^+ \to 0^+$
14	1434	58,60,62,64	^{52}Cr	$2^+ \to 0^+$
15	1440[a]	58,62	^{53}Mn	$? \to \frac{7-}{2}$
16	1454	58,60,62	^{58}Ni	$2^+ \to 0^+$
	1482	58,62	^{51}Cr	$? \to \frac{7-}{2}$
17	1524	58	^{42}Ca	$2^+ \to 0^+$

[a] Not completely resolved from an adjacent line. The division of strength between lines was estimated.

[b] This line was obscured by the ^{62}Ni $4^+ \to 2^+$ γ ray from the ^{62}Ni and ^{64}Ni targets.

[c] This line is not resolved from the 1173–keV ^{60}Ni $4^+ \to 2^+$ line. An estimated strength for the ^{60}Ni γ ray was subtracted.

[d] There is a $\frac{7-}{2} \to \frac{3-}{2}$ transition in ^{55}Fe at the same energy whose strength can be inferred from another decay branch, $\frac{7-}{2} \to \frac{5-}{2}$, and then subtracted.

TABLE II. Cross section (in mb) for production of individual nuclides from Ni targets as determined from prompt γ-ray spectra.

Beam	π^+	π^-	π^+	π^-	π^+	π^-	π^+	π^-	π^+	π^-	π^+	π^-
Energy (MeV)	100	160	160	220	220	220	220	160	160	220	220	220
Target Nuclide	^{58}Ni[a]	^{58}Ni	^{58}Ni	^{58}Ni	^{58}Ni[a]	^{60}Ni[a]	^{60}Ni[a]	^{62}Ni	^{62}Ni	^{62}Ni	^{62}Ni[b]	^{64}Ni
^{64}Ni												(82)[c]
^{62}Ni								(89)[c]	(83)[c]	(131)[c]	(93)[c]	49
^{61}Ni								10	16	10	7	26
^{60}Ni						(99)[c]	(85)[c]	65	67	79	69	42
^{59}Ni						55	51	37	38	55	48	
^{58}Ni	(57)[c]	(83)[c]	(58)[c]	(70)[c]	(64)[c]	17	8	15	17	18	19	
^{57}Ni	9	15	6	13	7							
^{61}Co								19	18	21	23	21
^{60}Co[d]												9
^{59}Co						29	49	47	41	42	42	27
^{57}Co	36	44	44	45	61	50	55	25	37	32	38	27
^{56}Co[d]	31	25	22	33	30	4	8	12	7	15	10	7
^{58}Fe								32	30	34	28	46
^{56}Fe	26	52	38	37	26	85	48	80	82	103	75	46
^{55}Fe	90	98	88	91	87	76	79	34	59	48	52	25
^{54}Fe	34	58	58	32	47	14	18	17	22	20	20	
^{55}Mn[d]	14				9	8	12					
^{53}Mn		21	26	16				14	10	11	18	
^{52}Cr	20	23	23	32	20	45	38	50	41	43	34	43
^{51}Cr[d]		23	25	25				11	6	13	14	8
^{50}Cr	45	29	31	29	40	18	28	14	26	20	28	
^{51}V[d]								9	17	8	11	11
^{49}V[d]	20				28	23	24					
^{48}Ti	7	24	18	22	12	22	14	25	16	24	24	22
^{47}Ti	17	24	23	35	21	5	13	22	21	27	33	41
^{46}Ti	23	23	23	26	34	17	22	16	27	18	15	
^{45}Ti[d]	4				7							
^{44}Ca								11	16	13	16	
^{42}Ca	6	10	13	15	10							
	382	469	438	451	439	468	467	565	614	654	624	450

[a] From Ref. 5.

[b] There is an uncertainty in the absolute normalization of this column as discussed in the text.

[c] May be dominated by secondary processes. Inelastic-scattering cross sections were not used in determining total cross sections or averaged values.

[d] Only a single line was observed and therefore the identification of these nuclei must be regarded as less certain.

dary reactions. Secondary (n,p) and (n,α) reactions could be contributing as much as 10–20 mb of the observed cross sections with the ^{58}Ni target, with the yield diminishing for the heavier isotopes where these reactions are more endoergic. A rough estimate from recent measurements[12] of π^+ inelastic scattering indicates that the cross section for exciting all bound states in ^{58}Ni is about 75 mb at $E_\pi = 162$ MeV.

At the end of the 220-MeV π^+ measurement on ^{62}Ni, it was noticed that the LEP channel settings had drifted somewhat and the beam may not have been fully intercepted by the target. When the data from this run were normalized in the same manner as the other measurements, the resultant cross sections were found to be lower than the other measurements on ^{62}Ni (at the other energies and with π^-) by an average factor of 1.7. Since it is not possible to correct the normalization for the drift in the pion channel, the cross sections were multiplied by 1.7 to give best overall agreement with the other ^{62}Ni data. Hence the absolute cross sections for this run are not well determined. However, the normalization uncertainty does not effect relative cross sections and the mean nucleon removal number derived from them.

The level scheme of the final nuclides plays an important role in determining how easily each

species are observed. Excluding inelastic scatter-ing, the observed prompt γ rays account for 500 to 600 mb of the total cross section. Most parti-cle-stable levels formed in even-even nuclei can be expected to decay by cascades leading eventually to the first-excited state, particularly since the evaporation process tends to favor higher-spin states. Thus the yield of γ rays from the first-excited state is a good measure of the total yield for an even-even nucleus. In contrast, there are likely to be many competing, more complex, decay modes when an odd-odd nucleus is formed, and much of the yield may be missed. Only two odd-odd nuclides (both Co isotopes) were seen in the prompt γ rays from Ni targets. It is not obvious why only one line out of several possible ones was seen for ^{60}Co, though most of these other transi-tions fall in the energy below 511 keV where the background is higher.

In odd-A nuclei one may sometimes observe the important decay modes. Unlike the even-A nuclei, there is no simple rule to predict which line will be strongest. A search was made for the expected odd-A nuclides for all the low-lying transitions with known large branching ratios. Several transitions were seen from states of spin $\frac{9}{2}$ or $\frac{11}{2}$, but some transitions were also seen from low-spin states. Which transitions are strongest presumably depends on details of nuclear structure and level ordering. Because of the dif-ficulty in predicting which lines will be most in-tense, the observation of only one γ-ray line from an odd-A nucleus does not identify the presence of that nuclide as certainly as does a $2^+ \to 0^+$ transi-tion in an even-even nucleus. Such cases are iden-tified in Table II. Since weak branches were fre-quently not observable, each measured γ-ray in-tensity was divided by the known branching ratio in arriving at the entries for Table II.

An off-line Ge(Li) spectrometer system was used to measure the radioactivities induced by the bom-bardment of ^{58,60,62}Ni targets with 220-MeV π^- and a ^{62}Ni target with 220-MeV π^+. Counting started a few minutes after the end of bombardment and con-tinued for up to about 200 days. The observed count rates were converted to disintegration rates using empirically determined efficiencies and cor-rections for the source dimensions, absorption in the thick source, and coincident γ-ray summing. Formation cross sections were calculated using the measured beam exposure and the branching ratio for each γ ray in the decay. The absolute cross sections are uncertain to about 20%, because of uncertainties in the various corrections.

The measurements of these β-delayed γ-ray spectra provide information complementary to the prompt γ spectrum. The results of the radioactiv-

TABLE III. Cross sections in mb for the production of individual radionuclides.

Beam:	π^-	π^-	π^-	π^+
Energy: (MeV)	220	220	220	220
Target:	^{58}Ni	^{60}Ni	^{62}Ni	^{62}Ni
Nuclide				
^{57}Ni	89	4.7	1	1.2
^{56}Ni	7			
^{61}Co			31	(44)
^{58}Co		67	65	84
^{57}Co		87	43	64
^{56}Co	83[a]	30	14	22
^{55}Co	27	5.4	2	2.6
^{59}Fe			12	10
^{53}Fe	18	2.7	4	4
^{52}Fe	3.0	0.6		0.4
^{56}Mn		4.8	14	11
^{54}Mn	40	53	54	59
^{52m}Mn	15[b]	7.5[b]		5.6[b]
^{52}Mn	36	22	14	17
^{51}Cr	110	81	40	60
^{49}Cr	38	15	3	12
^{48}Cr	3.1	0.9		0.6
^{48}V	38	26	11	17[c]
^{48}Sc	0.4	0.9		0.8
^{47}Sc	2.2	6	5	4.6
^{46}Sc	11	13		8
^{44m}Sc	13	7.5		5
^{44}Sc	11	6	5	4
^{43}K	0.8	1.4		0.9
^{42}K	3.5	3		
	549	445	318	438

[a] ^{56}Ni subtracted.
[b] ^{52}Fe subtracted.
[c] ^{48}Cr subtracted.

ity measurements are listed in Table III. Com-parison with Table II for the same target and beam conditions shows that only a few nuclides are ob-served in both spectra and in these cases, as ex-pected, the activity measurement gives the larger cross section. For all of the targets studied al-most all of the activity was from odd-even or odd-odd nuclei although activity from three even-even nuclei, ^{56}Ni, ^{52}Fe, and ^{48}Cr, was observed. These nuclei are all rather far from the line of stability and were produced with cross sections that are so small that even the γ rays from the decay of their first excited state would have been missed in the prompt spectra.

When the prompt and delayed γ-ray measure-ments are combined the total cross section amounts to ~900 mb of reaction strength. Com-bined data for 220-MeV $\pi^\pm$ on ^{62}Ni are shown in Fig. 2. The wide range of final nuclides and their
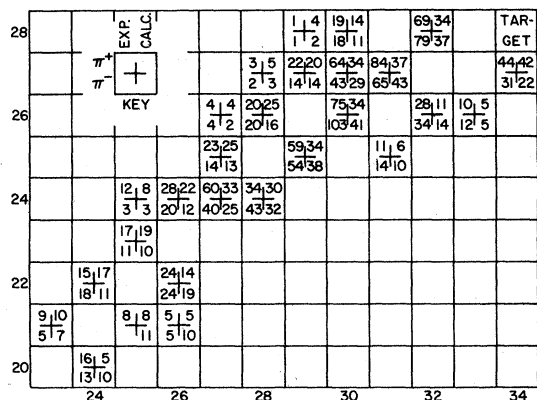
FIG. 2. Measured and calculated cross sections for producing observable even Z, even N, and radioactive nuclei from a ^{62}Ni target by 220-MeV π^+ and π^- beams.

FIG. 3. Nuclide production cross sections for (a) 220-MeV π^- on ^{58}Ni, (b) 220-MeV π^- on ^{60}Ni, (c) 220-MeV π^- on ^{62}Ni, and (d) 220-MeV π^+ on ^{62}Ni as a function of A. The cross sections for all isobars observed in the prompt and delayed γ spectra have been summed to give each solid or open circle; the latter symbol is used for those A values for which a significant amount of cross section is likely to have been missed. The triangles show the results of the cascade calculation including only the observed nuclides, with open triangles used for those A values where a substantial portion of the yield is believed to be in nuclides not observed. The solid lines indicate the trends in the data, the dashed lines in the calculations.

tendency to cluster along the valley of stability are evident. The cross sections for producing each value of A are shown in Fig. 3.

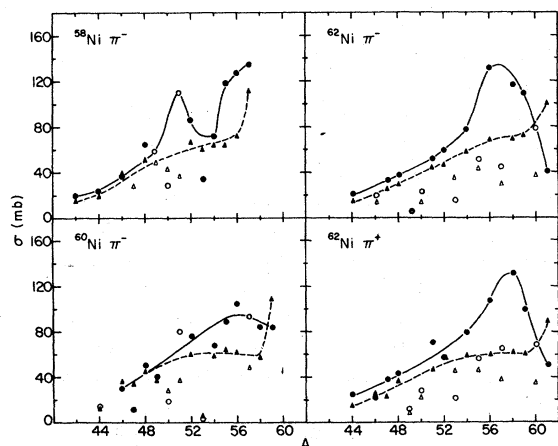It is apparent that much of the cross section that was missing in the prompt measurements for odd-odd final nuclides does show up in the activation data. The results, therefore, are more-or-less complete for the even-A chains. For the odd-A nuclides there is still often a problem, in that the prompt γ-ray cascades may be too complicated to show up in the measurements, and the residual nucleus may be stable, as for ^{57}Fe and ^{55}Mn, or the lifetime too short for the activation measurements, as for ^{57}Mn or ^{55}Cr. It is interesting to note in this context that in Fig. 3 the points fall below a smooth trend mostly for the odd-A values (53, 55, 57) where it is likely that some of the isotopes expected to be populated with large yields were not identified; These points are shown as open circles. A similar problem occurs for $A = 50$, where the systematics presented in Fig. 3 suggest significant strength for ^{50}V, an odd-odd nucleus with too long a lifetime ($\sim 6 \times 10^{14}$ years) to be seen in the activation measurements.

III. DISCUSSION OF RESULTS

Where radioactivities were measured, the total observed cross section is about 900 mb, exclusive of inelastic scattering, while, if optical-model parameters obtained from fits to 162-MeV elastic-scattering data[12] are used, reaction cross sections of about 1100 mb are calculated. If one were to assume that the evaporation residues are smoothly distributed in A and that for each value of A the proper cross sections are those represented by the smooth curves in Fig. 3, one obtains total cross sections of $\sim$1200 mb. This smoothing may be qualitatively justified, as was discussed in the preceding section, because the yield for several stable odd-A nuclei could not be readily extracted from the γ-ray spectra.

To parametrize the overall trend in the distribution of evaporation residues two quantities have been computed. One is the average number of nucleons removed, $\langle \Delta A \rangle$, which is simply the difference between the atomic weight of the target and the cross-section-weighted average atomic weight of evaporation residues. To get a measure of the distribution of yield among the different isotopes, the difference between the average number of removed neutrons and protons is also tabulated in the form $\langle \Delta N \rangle - \langle \Delta Z \rangle$, where

$$\langle \Delta A \rangle = A_T - (\textstyle\sum \sigma_i A_i)/(\textstyle\sum \sigma_i) \text{ and}$$

$$\langle \Delta N \rangle - \langle \Delta Z \rangle = N_T - Z_T - [\textstyle\sum \sigma_i (N_i - Z_i)]/(\textstyle\sum \sigma_i) ,$$

where the subscript T refers to the target and i to the various residual nuclides.

The total cross sections observed are tabulated for the Ni isotopes in Table IV and the comparisons in $\langle \Delta A \rangle$ and $\langle \Delta N \rangle - \langle \Delta Z \rangle$ are made in Table V. It can be seen that inclusion of the results of activation measurements does not modify the values of

TABLE IV. Summary of total observed cross sections. For comparison data from proton bombardment, Ref. 8, are also given. The underlined values include radioactivity measurements while for the others only prompt spectra were taken.

	^{58}Ni	^{60}Ni	^{62}Ni	^{64}Ni
45-MeV π^-[a]	502	598	525	
100-MeV π^+	382			
160-MeV π^-	469		565	
160-MeV π^+	438		614	
220-MeV π^-	929, 451	859, 468[b]	891, 654	450
220-MeV π^+	439[b]	467[b]	977, 624	
80-MeV p[c]	606, 432		530, 426	
100-MeV p[c]	466	555	435	529
136-MeV p[c]	435	509	570, 463	508
164-MeV p[c]	522, 352		587, 466	

[a] From Ref. 13.
[b] From Ref. 5.
[c] From Ref. 8.

TABLE V. Comparison of the values of $\langle \Delta A \rangle$ and $\langle \Delta N \rangle - \langle \Delta Z \rangle$ for the Ni isotopes. The underlined values are those where the radioactivity data was added in. Otherwise only prompt spectra were available.

| Beam	^{58}Ni	^{60}Ni	^{62}Ni	^{64}Ni
		$\langle \Delta A \rangle$		
Stopped π^-[a]		3.9	4.8	5.8
45-MeV π^-[a]		3.8	4.9	5.7
100-MeV π^+		5.1		
160-MeV π^-		5.2		6.9
160-MeV π^-		4.9		6.7
220-MeV π^+		5.4	5.5[a]	7.2, 6.9
220-MeV π^-	5.6, 5.4[a]	6.1, 5.3[a]	6.8, 6.6	7.8
80-MeV p[b]	3.2, 3.3		3.3, 3.4	
100-MeV p[b]		3.6	2.8	3.7 3.5
136-MeV p[b]		4.1	3.5	4.3, 4.5
164-MeV p[b]	4.2, 4.5		4.7, 5.0	
		$\langle \Delta N \rangle - \langle \Delta Z \rangle$		
Stopped π^-[a]		−0.9	0.0	1.4
45-MeV π^-[a]		−1.2	0.3	1.5
100-MeV π^+		−0.8		
160-MeV π^+		−0.8		2.3
160-MeV π^-		−0.8		2.2
220-MeV π^+		−0.7	0.7[a]	2.3, 2.3
220-MeV π^-	−0.4, −0.8[a]	0.8, 0.7[a]	2.2, 2.3	3.5
80-MeV p[b]	−0.3, −0.5		1.8, 1.8	
100-MeV p[b]		−0.5	0.7	1.9 2.6
136-MeV p[b]		−0.6	0.7	1.9, 2.0 2.8
164-MeV p[b]	−0.5, −0.6		1.9, 1.9	

[a] Ref. 13.
[b] Ref. 8.
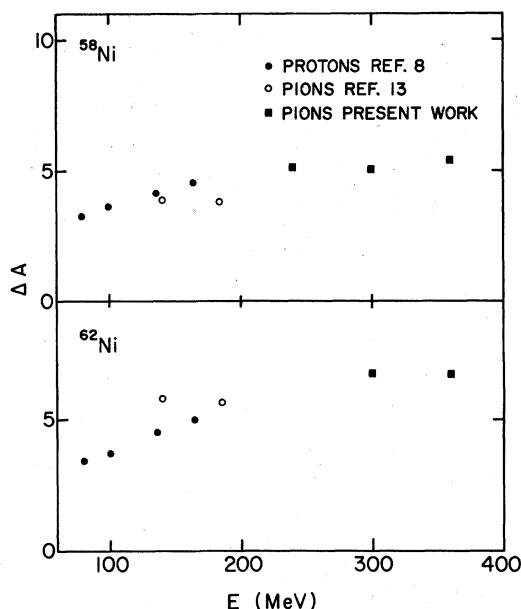
FIG. 4. The average number of nucleons removed from pion and proton measurements as a function of energy. The pion's rest mass is included in the energy, the proton's is not. On the other hand, the proton is included in computing $\langle \Delta A \rangle$; here $\langle A \rangle \equiv (A_T + 1) - (\sum \sigma_i A_i / \sum \sigma_i)$.

$\langle \Delta A \rangle$ and $\langle \Delta N \rangle - \langle \Delta Z \rangle$ appreciably. The uncertainties in Table IV are not easy to estimate; they are probably less than ~0.3. Plots of $\langle \Delta A \rangle$ as a function of incident energy are given in Fig. 4. Some trends in the Ni data can be best seen by graphing the average neutron and proton removal numbers as vectors leaving the target in the N-Z plane. Because of the observed independence to pion charge and energy, the nucleon removal vectors were averaged over all measurements on a given target for display in Fig. 5. It is apparent that these vectors point toward the valley of stability.

Since the same selection of final nuclides is studied with the same experimental technique for all the Ni isotopes, systematic trends in these quantities appear to be a meaningful probe of the reaction mechanisms. A number of qualitative points may be noted.

1. The gross features of the distribution of evaporation residues, as reflected by the values of $\langle \Delta A \rangle$ and $\langle \Delta N \rangle - \langle \Delta Z \rangle$ are remarkably independent of pion energy in this energy region. This independence perhaps suggests that absorption may play a major role in the pion-nucleus interaction. As can be seen in Fig. 4, recent results[13] with stopped and 45-MeV π^- indicate a slight decrease
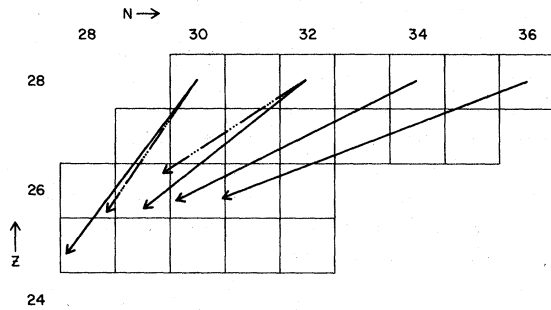
FIG. 5. Mean proton and neutron removal numbers displayed as vectors in N-Z space. The energy- and pion-charge-averaged values for pion beams are shown as solid lines; the values for protons from Ref. 8 are drawn as dot-dashed lines.

FIG. 6. Same as Fig. 3 for 164-MeV p on (a) ^{58}Ni and (b) ^{62}Ni. The experimental data are from Ref. 8; open circles are used for all odd masses, regardless of the likelihood of missed cross sections. The squares are the summed calculated cross sections, with the lines indicating the approximate trend in the calculations.

in $\langle \Delta A \rangle$ at lower energies.

2. The bulk of the cross sections, as reflected in $\langle \Delta N \rangle - \langle \Delta Z \rangle$ for instance, are remarkably insensitive to pion charge. On the other hand, the centroid of evaporation residues changes with neutron excess, as is clear in Fig. 5; the "compound system" with $\pi^+ + {}^{62}\text{Ni} \rightarrow {}^{62}\text{Cu}$ or with $\pi^- + {}^{62}\text{Ni} \rightarrow {}^{62}\text{Co}$ has a neutron excess of four in the first case and eight in the second. Thus, the end products of the reaction do reflect in some manner the isospin of the target, but they do *not* reflect the charge of the incident pion. On the average, the charge of the pion seems to be removed in the early preequilibrium stage of the reaction and the excited system that is left to evaporate is the same, regardless of the incident pion's charge. While this is true of the bulk of the cross section, individual nuclides, generally with a small fraction of the total yield, still show large π^+/π^- values, e.g., ^{56}Co or ^{48}Cr, especially when $\langle \Delta N \rangle - \langle \Delta Z \rangle$ is far from its average value.

3. The change in $\langle \Delta A \rangle$ and in $\langle \Delta N \rangle - \langle \Delta Z \rangle$ with increasing neutron excess of the target arises largely from an increase in $\langle \Delta N \rangle$, while $\langle \Delta Z \rangle$ remains rather constant at about 2.5 nucleons. This may reflect the weaker binding of neutrons in the heavier Ni isotopes.

4. A striking feature of the final mass distributions is the large yield of nuclides that are a few nucleons removed from the target. This effect is most dramatic for the ^{62}Ni target where the resultant distribution exhibits a large peak at about $A = 58$. For the ^{58}Ni target, the cross sections for nuclei 1–3 nucleons removed are large (the "unobservable" ^{57}Fe and ^{55}Mn are not along the evaporation chain here) and there is a secondary peak at $A = 51$ ($\Delta A = 7$). The distribution for a ^{60}Ni target lies in between those for ^{58}Ni and ^{62}Ni.
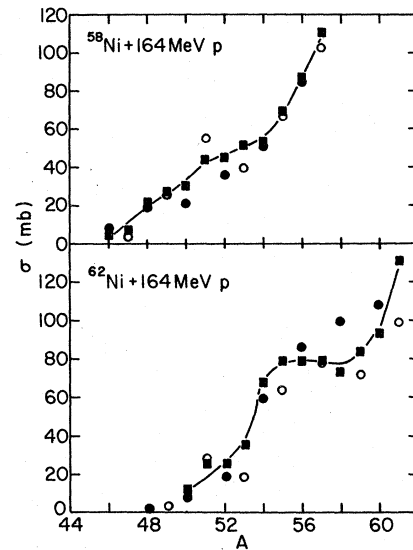
The mass distribution is qualitatively different with proton bombardment. For ^{58}Ni and ^{62}Ni it can be seen in Fig. 6 that the cross sections fall off rather smoothly with the number of removed nucleons. Since the proton experiments[8] were done with a primary beam the experimental conditions were very much better and many more weak transitions could be identified. Several other differences between the pion and the proton data are noteworthy:

(a) The cross section for producing the same set of final nuclides is larger for pions than for protons of the same kinetic energy. This suggests that nuclei are more transparent for protons than for pions, as expected, since the π-nucleon cross section in this energy region is larger than the corresponding nucleon-nucleon cross section.

(b) For protons on a given target, the average number of nucleons removed increases with increasing bombarding energy. If the pion rest energy is included and the proton is added to A_T in computing $\langle \Delta A \rangle$, the number of nucleons removed as a function of incident particle energy falls on a smooth curve which flattens out at about 200–250 MeV (Fig. 4).

(c) The nucleon removal number $\langle \Delta A \rangle$ changes less than half as much with target neutron excess for proton bombardment, as it does with pions. On the other hand, the increase of $\langle \Delta N \rangle - \langle \Delta Z \rangle$ with in-

creasing target neutron excess is comparable in the two cases.

The only model calculations that attempt to fit such data are Monte Carlo calculations,[14,15] in which the pion is allowed to scatter from the nucleons in the nucleus with the free pion-nucleon cross section. The Δ resonance, when formed, is allowed to interact with another nucleon, and thereby provide a mechanism for pion absorption. Any nucleons that acquire momenta above the Fermi momentum are allowed to cascade with the free nucleon-nucleon cross sections. The computer program of Ref. 14 has been modified extensively by Ginocchio[15] to include a number of additional effects, such as an energy-dependent lifetime of the Δ, refraction of pions and nucleons at the nuclear surface, and others. Figure 2 displays the experimental and the calculated cross sections for ^{62}Ni isotope by isotope for both π^+ and π^-. Some differences are apparent, others are not so clear. Perhaps the plot of summed cross sections shown in Fig. 3 is more informative. The predicted cross sections for producing nuclides 2–7 nucleons removed from the target are too low by as much as a factor of 2. On the other hand, the predicted increase in yield for one nucleon removal is not observed. For example, ^{51}Cr was found to be produced from ^{58}Ni with a cross section of 110 mb while the calculation predicts the ^{51}Cr + ^{51}Mn production cross section to be 55 mb. Similarly, the cross section for producing ^{56}Fe from ^{60}Ni was 85 mb while the prediction is 29 mb. The formation of nuclides farther away from the target in nucleon number are reproduced reasonably well. The large discrepancy for nearby nuclides causes the observed cross section to be about 200 mb greater than the predicted one for producing the same set of nuclei even though, in the prompt spectra, some of the cross section may have been missed.

The same code has been used to predict the production cross sections for protons bombarding the various nickel targets; the same options and parameters were used as for the pions.[16] These predictions for the mass spectra are compared with the experimental results in Fig. 3. The agreement is very good, even for removing a small number of nucleons from the target. Thus, the cascade-evaporation calculation does appear to reproduce the inclusive features of nucleon-produced reactions in this energy range (see Table VI). The failure to reproduce the nuclide mass spectrum from pion initiated reactions, therefore, may be attributed to a lack of understanding of the *pion*-nucleus interaction.

The cascade calculations also had difficulties in reproducing some features of the energetic proton yields[7] from pion bombardment. The predicted cross sections were usually too small, in some cases by as much as a factor of 3, and the observed A-dependence was not reproduced well. The fact that the mass spectrum for removing more than ≈ 8 nucleons is well reproduced by the intranuclear cascade code implies that the evaporation phase is correctly handled. In this part of the calculation nucleons and α particles are boiled off using standard nuclear statistical theories.

Inelastic pion scattering, with the nucleus sufficiently excited so as to emit several nucleons, may explain the large yield of nuclides a few nucleons removed from the target. Unfortunately, there appear to be no published inelastic scattering data on which to base an estimate of the importance of such a process.

Spectra from the $(\pi^\pm, \pi^0)$ charge exchange reaction show the π^0 yield extending to a very low π^0 energies with the average about $\frac{1}{2}$ the initial kinetic energy.[17] Data were taken at only 40 and 140°, but if the angular distribution were to be smoothly in-

TABLE VI. Comparison of summed cross sections and mean removal numbers between experiment and cascade-evaporation calculations. Only those cases where radioactivities were measured are considered and the comparison includes only the experimentally observed nuclides. The proton data are from Ref. 8.

Target	Beam	Energy MeV	σ (mb) Exp.	σ (mb) Calc.	$\langle \Delta A \rangle$ Exp.	$\langle \Delta A \rangle$ Calc.	$\langle \Delta N \rangle - \langle \Delta Z \rangle$ Exp.	$\langle \Delta N \rangle - \langle \Delta Z \rangle$ Calc.
^{58}Ni	π^-	220	929	662	5.6	5.6	−0.4	−0.3
^{60}Ni	π^-	220	859	712	6.1	6.6	0.8	1.1
^{62}Ni	π^-	220	891	695	6.8	6.8	2.2	2.2
^{62}Ni	π^+	220	977	759	7.1	7.5	2.3	2.7
^{58}Ni	p	80	606	599	3.2	3.1	−0.3	0.1
^{58}Ni	p	164	522	571	4.2	4.5	−0.5	0.0
^{62}Ni	p	80	530	619	3.3	3.8	1.8	2.3
^{62}Ni	p	136	570	616	4.3	4.8	1.9	2.3
^{62}Ni	p	164	587	617	4.7	5.1	1.9	2.3

terpolated, the total cross section for nickel would be ≈120 mb. Since in the region dominated by the Δ resonance, elastic pion-nucleon scattering should be five times as great as charge exchange, perhaps as much as 600 mb of large-momentum-transfer pion-nucleus inelastic scattering could be taking place. However, until inelastic spectra are actually measured, the importance of inelastic scattering in pion-induced reactions must remain conjectural.

V. CONCLUSION

The distribution of residual nuclides left after pion-induced reactions on the Ni isotopes shows a consistent systematic pattern which differs qualitatively from proton-induced reactions in several respects. The spectrum of residual nuclides following pion bombardment is very sensitive to target isospin, but independent of beam isospin or energy. Whatever the mechanisms, for the major fraction of the reactions the incident pion's charge seems to be removed at the precompound stages of the process. Most of the yield is concentrated in nuclei between 2 and 7 nucleons lighter than the target, while pion-induced nucleon knockout is a rather weak and unimportant process. There does not seem to be any preferential removal of α particles in the latter stages of the reaction.

*Present address: Technical University of Munich, West Germany.

†Also at the University of Chicago, Chicago, Illinois 60637.

‡Present address: University of Maryland, College Park, Maryland 20742.

§Present address: Indiana University, Bloomington, Indiana 47401.

‖Now at Argonne National Laboratory, Argonne, Illinois 60439.

**Also at Argonne National Laboratory.

[1]P. D. Barnes, R. A. Eisenstein, W. C. Lam, J. Metler, R. B. Sutton, M. Eckhause, J. Kane, R. E. Welsh, D. A. Jenkins, R. J. Powers, R. Kunselman, R. P. Redwine, R. E. Segel, and J. P. Schiffer, Phys. Rev. Lett. 29, 290 (1972).

[2]V. G. Lind, H. S. Plendl, H. O. Funsten, W. J. Kossler, B. J. Lieb, W. F. Lankford, and A. J. Buffa, Phys. Rev. Lett. 32, 479 (1974).

[3]R. E. Segel, L. R. Greenwood, P. Debevec, H. E. Jackson, D. G. Kovar, L. Meyer-Schützmeister, J. E. Monahan, F. J. D. Serduke, T. P. Wangler, W. R. Wharton, and B. Zeidman, Phys. Rev. C 13, 1566 (1976).

[4]O. Artun, Y. Cassagnou, R. Legrain, N. Lisbona, L. Roussel, J. P. Alard, A. Baldit, J. P. Cosilhes, J. Fargeix, G. Roche, and J. C. Tamain, Phys. Rev. Lett. 35, 773 (1975).

[5]H. E. Jackson, D. G. Kovar, L. Meyer-Schützmeister, R. E. Segel, J. P. Schiffer, S. E. Vigdor, T. P. Wangler, R. L. Burman, D. M. Drake, P. A. M. Gram, R. P. Redwine, V. G. Lind, E. N. Hatch, O. H. Otteson, R. E. McAdams, B. C. Cook, and R. B. Clark, Phys. Rev. Lett. 35, 641 (1975).

[6]D. Ashery, M. Zaider, Y. Shamai, S. Cochabi, M. A. Moinester, A. C. Yavin, and J. Alster, Phys. Rev. Lett. 32, 943 (1974).

[7]H. E. Jackson, S. B. Kaufman, L. Meyer-Schützmeister, J. P. Schiffer, S. L. Tabor, S. E. Vigdor, J. N. Worth-ington, L. L. Rutledge, Jr., R. E. Segel, R. L. Burman, P. A. M. Gram, R. P. Redwine, and M. A. Yates, Phys. Rev. C 16, 730 (1977); H. E. Jackson, S. L. Tabor, K. E. Rehm, J. P. Schiffer, R. E. Segel, L. L. Rutledge, Jr., and M. A. Yates, Phys. Rev. Lett. 39, 1901 (1978).

[8]M. Sadler, J. Jastrzebski, A. Nadasen, P. P. Singh, L. L. Rutledge, Jr., T. Chen, and R. E. Segel, Phys. Rev. Lett. 38, 950 (1977); and M. Sadler, Ph.D. Thesis, Indiana University, 1977 (unpublished).

[9]H. E. Jackson, D. G. Kovar, L. Meyer-Schützmeister, S. E. Vigdor, T. P. Wangler, R. E. Segel, J. P. Schiffer, R. L. Burman, P. A. M. Gram, D. M. Drake, V. G. Lind, E. N. Hatch, O. H. Otteson, R. E. McAdams, B. C. Cook, and R. B. Clark, Phys. Rev. Lett. 35, 1170 (1975).

[10]B. J. Dropesky, G. W. Butler, C. J. Orth, R. A. Williams, G. Friedland, M. A. Yates, and S. B. Kaufman, Phys. Rev. Lett. 34, 821 (1975).

[11]T. P. Wangler and S. E. Vigdor, Nucl. Instrum. Methods 129, 437 (1975).

[12]B. Zeidman, C. Olmer, D. F. Geesaman, R. L. Boudrie, R. H. Siemssen, J. F. Amann, C. L. Morris, H. A. Thiessen, G. R. Burleson, M. J. Devereux, R. E. Segel, and L. W. Swenson, Phys. Rev. Lett. 40, 97 (1978).

[13]Y. Cassagnou, H. E. Jackson, J. Julien, R. Legrain, L. Roussel, S. Barbarino, and A. Palmeri, Phys. Rev. C 16, 741 (1977).

[14]G. D. Harp, K. Chen, G. Friedlander, Z. Fraenkel, and J. M. Miller, Phys. Rev. C 8, 581 (1973).

[15]J. Ginocchio, Phys. Rev. C 17, 195 (1978); and private communication.

[16]We thank T. Chen for making these calculations available to us.

[17]T. Bowles, D. F. Geesaman, R. J. Holt, H. E. Jackson, R. M. Laszewski, J. R. Specht, L. L. Rutledge, Jr., R. E. Segel, R. P. Redwine, and M. A. Yates-Williams, Phys. Rev. Lett. 40, 97 (1978).